

New Efficient Filter Design for a Heat Sink

J. Kulanayagam, J. H. Hagmann, K. F. Hoffmann and S. Dickmann

Helmut-Schmidt-University / University of the Federal Armed Forces Hamburg
Holstenhofweg 85, 22043 Hamburg (Germany)

Phone: +49 40 6541 2587, Fax number: +49 40 6541 2018

E-mail: Kulanayagam@hsu-hh.de, Johannes.Hagmann@hsu-hh.de, Klaus.Hoffmann@hsu-hh.de,
Stefan.Dickmann@hsu-hh.de

Abstract. The heat sink design of a Switching Mode Power Supply influences the EMC of the supply. The capacitive coupling between electronic power device and the heat sink are responsible for common-mode currents in the system. These currents create EMC problems. This paper proposes a new filter design to avoid heat sink radiation. Experimental results validate the proposed filter.

Keywords

Switching Mode Power Supply, MOSFET, Heat Sink, Radiated Emission, Ferrite Core.

1. Introduction

Heat sinks are one of the main EMI sources in Switching Mode Power Supply (SMPS) due to capacitive coupling. Therefore, their shape and dimensions play a big role for the electromagnetic field radiation. Heat sinks should be well designed to ensure compliance with the EMC standards.

The heat sink current depends prevalently on a parasitic capacitance and the drain-source voltage variation. The decrease in commutation time and the increase of the insulation voltage of the power electronic components lead to an increase of the time derivative of the voltage. In consequence, the heat sink generates wide-band interference spectra [1, 2, 3].

The first part of this paper investigates the main concepts of common-mode EMI sources generated by SMPS. The second part concerns filter modelling to reduce EMI radiated emission of ungrounded heat sinks. The third part deals with an experimental setup for measuring the input impedance and the heat sink radiation.

2. EMI Sources and Electromagnetic Radiation

Power electronic semiconductors are generally mounted on heat sinks to drain the produced heat. A parasitic capacitance exists between the case of the semiconductor and the heat sink. The insulating thermal compound is the dielectric for this capacitor. It is shown as isolator 1 in Fig. 1.

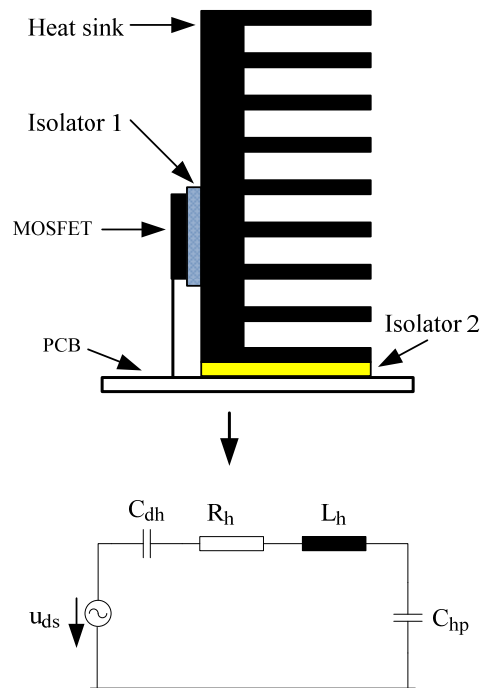


Figure 1 Schematic representation of parasitic capacitance and equivalent circuit

The typical common-mode current paths are described in [4]. If the heat sink is grounded, the common-mode currents to the SMPS increase [5]. In other words, the conducted EMI raises. If the heat sink is not grounded, the common-mode currents to the SMPS decrease, but the heat sink can become a highly efficient antenna emission when EMI resonant phenomena occur. The common-mode current paths are shown in Fig. 2.

The current path i_c via C_{hg} and ground represents the common-mode current and the current path i_h via C_{hp} and the PCB is the heat sink current. The common-mode current i_c produces conducted EMI, while i_h generates radiated EMI via the heat sink as an antenna. These currents can be calculated according to the following equation as a first approach for low frequencies

$$i_h(t) + i_c(t) = C_{dh} \cdot \frac{du_{ds}(t)}{dt} \quad (1)$$

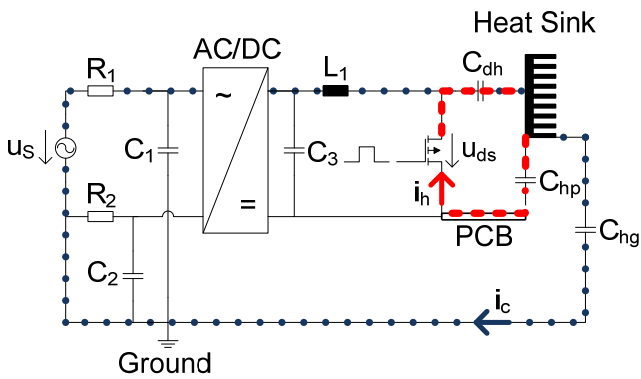


Figure 2 Common-mode current paths through heat sink in an AC/DC converter

The parasitic capacitance C_{dh} exists between the MOSFET and the heat sink. C_{dh} can reach approximately 100pF [4]. Other parasitic capacitances are smaller than C_{dh} . For that reason, only C_{dh} is considered. The time derivative of the drain-source voltage is du_{ds}/dt .

The stray capacitance between the transistor and the heat sink can be minimized by applying a screen between the transistor metal casing and the heat sink (Fig. 3). The sides of the screen are insulated with dielectric material. The characteristics of the screen and the dielectric material should provide a good thermal conductivity [6].

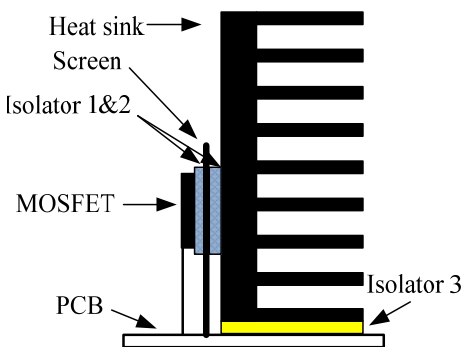


Figure 3 Reduction of the common-mode current by screening

The disadvantages of this model are not only the enhancement of the heat transfer resistance between the transistor and the heat sink. Also the circuit acts like a high pass filter. High frequency currents can radiate via the heat sink. To solve this problem, the filter model for heat sink is introduced. In this paper the common-mode radiated EMI current loop between the heat sink and PCB (see Fig.2) is considered. This is again shown in Fig. 4

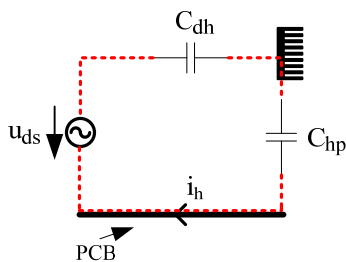


Figure 4 Common-mode current loop between the heat sink and the PCB

, where C_{dh} is the parasitic capacitance between the drain of the MOSFET and the heat sink and C_{hp} is the parasitic capacitance between the heat sink and the PCB.

3. Filter Design

Ferrite cores are usually attached to a cable or wire to suppress the electromagnetic noise emission from digital information equipment [7]. This idea is used in the heat sink model. The high magnitudes of disturbances due to the heat sink were attenuated and the high harmonic spectrums of heat sink currents were filtered. The block diagram of the filter model is shown in Fig. 5.

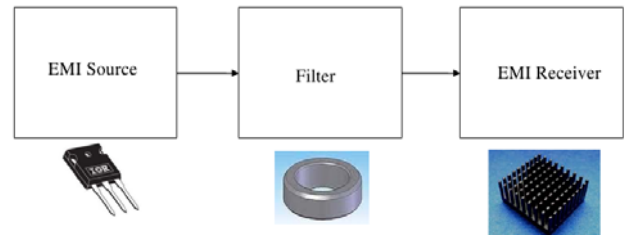


Figure 5 Block diagram of the filter model

A metal cylinder with similar material characteristics like the heat sink is fixed to the heat sink. A ferrite core is attached on the metal cylinder between heat sink and transistor. The new filter model is shown in Fig. 6. The main idea of this model is to reduce the high frequency current through the heat sink via ferrite cores. This current is given by

$$I_h = \frac{U_{ds}}{Z} \quad (2)$$

, where U_{ds} is the drain-source voltage of the transistor and Z is the impedance of the network.

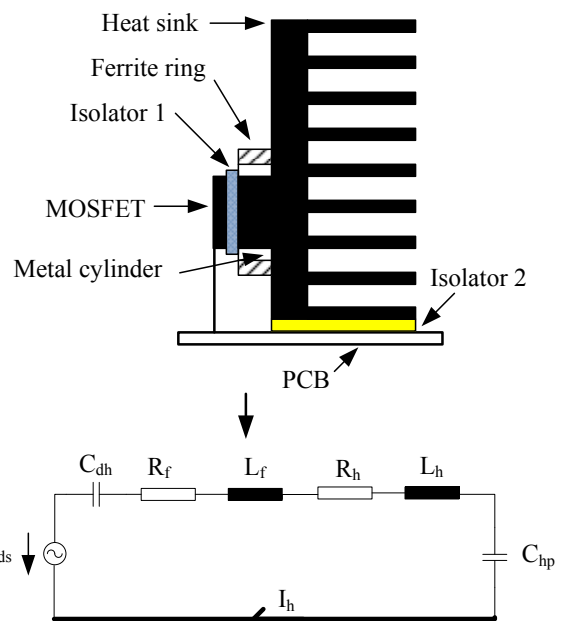


Figure 6 Schematic representation of the filter model and its equivalent circuit

The modified heat sink model changes are shown in Fig. 6. An additional resistor due to the frequency depending losses and an inductance have to be added in series to the first model of this resonant circuit.

The disadvantage of this model is a higher heat resistance as compared to the original setup. Yet this model has a lesser heat resistance than the screening model.

4. Experimental Setup

4.1 Input impedance of the heat sink

Heat sinks are good thermal conductors, and with the fins on the heat sink the effective cooling surface area is increased [8]. These fins and their dimensions and arrangement influence their electrical behaviour. Therefore, three different heat sinks were used to measure their input impedance. A first set of measurements was done as a reference for three different heat sink shapes with the same the dimensions but different fin arrangements. These geometric structures of heat sinks are shown in Fig.7, respectively.

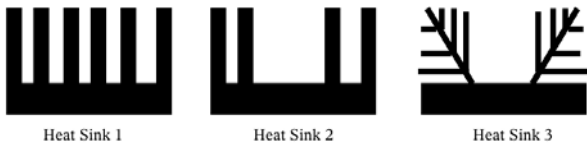


Figure 7 Geometric structures of heat sinks

The experiment setup for measuring the input impedance of these heat sinks is shown in Fig. 8.

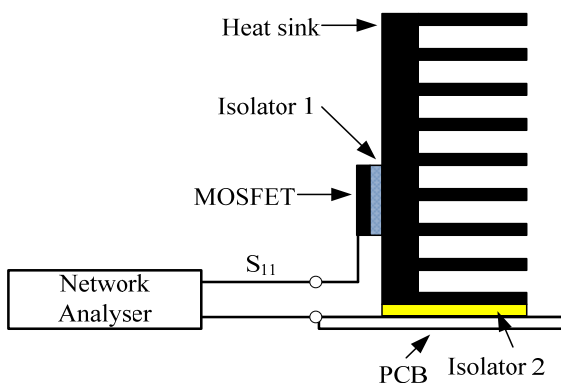


Figure 8 Measurement setup for the input impedance of the heat sinks

In a second step, we attached an extra metallic cylinder to the heat sink but did not add the ferrite core. A third measurement was done for a heat sink with three different ferrite cores. The measurement set up for the third configuration is shown in Fig. 9.

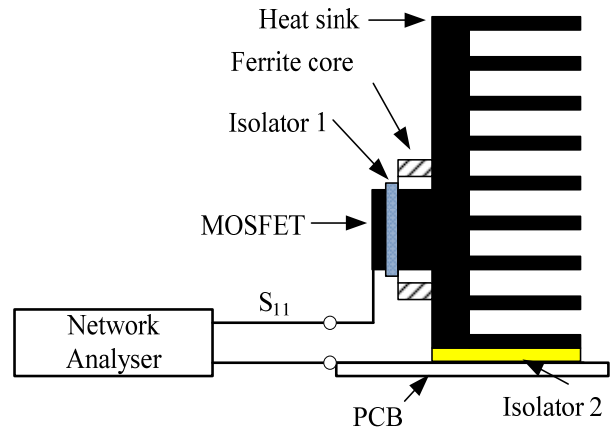


Figure 9 Measurement setup for the input impedance of the ferrite model

For the measurement a vector network analyser was used. It measures the scattering parameters S_{11} of the structure. From this, we get the input impedance of the network [9].

$$Z_{input} = 50\Omega \cdot \frac{1 + S_{11}}{1 - S_{11}} \quad (3)$$

In this work, the frequency range from 300 kHz up to 1 GHz was considered.

4.2 Radiation of the heat sink

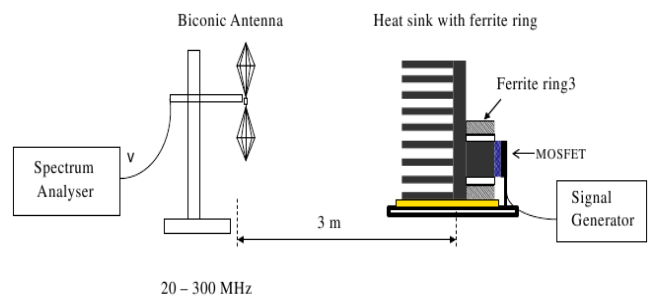


Figure 10 Measurement setup for radiation of the heat sink inside in an anechoic chamber

In order to validate the proposed heat sink ferrite model an experimental test was done inside an anechoic chamber. This was done to avoid the presence of environmental EMI noises in EMI measurements.

The RF signal generator was connected via a coaxial cable to the heat sink ferrite model. On the other side a biconical antenna receives the emitted electromagnetic fields from the heat sink. This received RF signal is detected by a spectrum analyser. In this work, the frequency range from 20 up to 300 MHz was considered.

The attenuation of the heat sink radiation is calculated with and without ferrite on the heat sink model. The measurement setups were configured for frontal and lateral radiation.

5. Results and Discussions

The measured impedance results for the first configuration are shown in Fig. 11. The curves of the input impedance of the three heat sinks show that the heat sink structures behave like series resonant circuits, as described the equivalent circuit in Fig. 1. Up to a resonant frequency f_{res} the impedance behaves like a capacitance and above the resonant frequency f_{res} the impedance behaves like an inductance. The following equation is used for the calculation of the resonant frequency of the input impedance

$$f_{res} = \frac{1}{2\pi\sqrt{L_{loop}C_{loop}}} \quad (4)$$

L_{loop} is the inductance of the current loop and C_{loop} is the capacitance of the current loop of the input impedance. All three heat sinks have the same values of the inductance L_{loop} because of the same current loop, which is spanned. But they have different values of the capacitance C_{loop} . That can be explained by the different values of the parasitic capacitive coupling between the heat sink and the PCB. C_{loop} depends on C_{dh} and C_{hp} . C_{dh} is the same for all three heat sinks but C_{hp} has different value for all three heat sinks because the fins of the heat sinks have different shape, as mentioned before (in Fig.7).

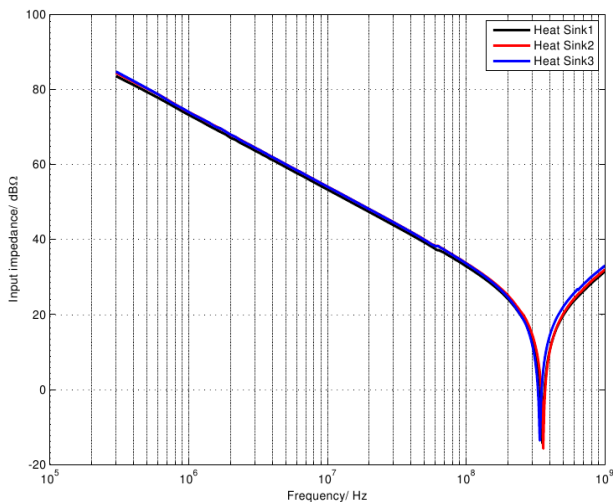


Figure 11 Input impedance of three different shaped heat sinks

In other words, these heat sinks have different contact areas between the heat sink and the PCB. That causes different parasitic capacitances C_{hp} . Therefore, all three heat sinks have different resonant frequencies. Fig. 12 shows an enlargement of the resonant frequency range displayed in Fig. 11. The resonant frequencies for the heat sink 1, the heat sink 2 and the heat sink 3 are 376 MHz, 405 MHz and 350 MHz, respectively.

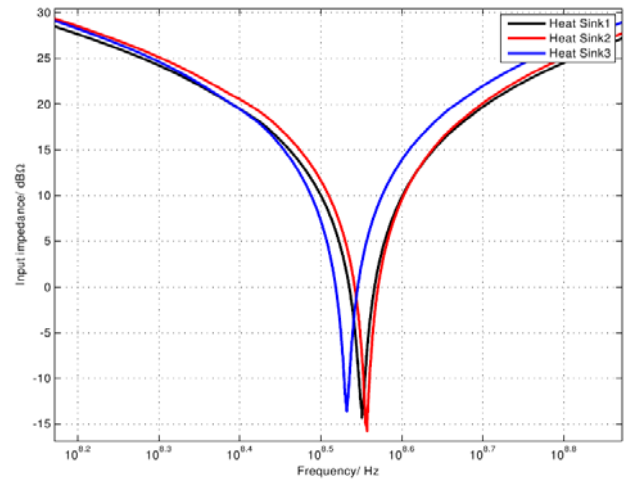


Figure 12 Enlarged curve of the Fig. 11 at the resonant frequency range

The results of the second and third configuration (using different ferrites) are shown in Fig. 13. The resonant frequency of the reference heat sink model was shifted down to the lower MHz frequency range because the extended heat sink model has a larger current loop than the reference model and a larger inductance. The capacitance values of the ferrite core models are identical at low frequencies. But at higher frequencies the inductance values of the ferrite models are different. This is because all three ferrite cores consist of different materials and therefore have different magnetic characteristics. The quality factors of the ferrite models are smaller than the quality factor of the reference model. This factor depends on the inductance of the ferrite cores.

The impedance of the ferrite heat sink model is increased because a ferrite core has a huge impedance, due to its permeability. This means that the heat sink currents will be minimized by putting the ferrite core between the heat sink and the transistor and the heat sink radiation is reduced by this filter.

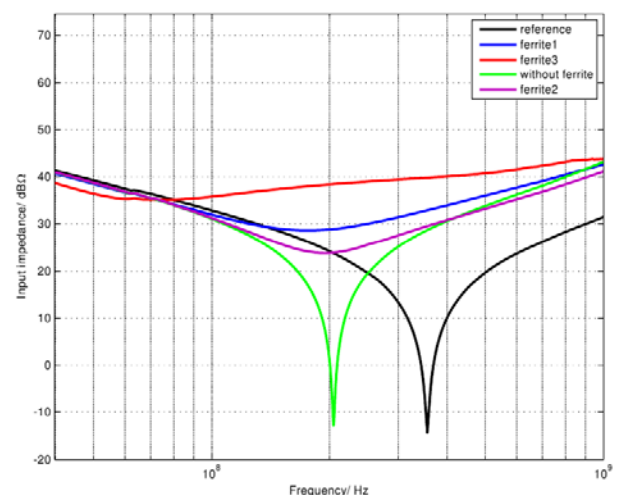


Figure 13 Impedance of the reference, enhanced heat sink with and without ferrite core

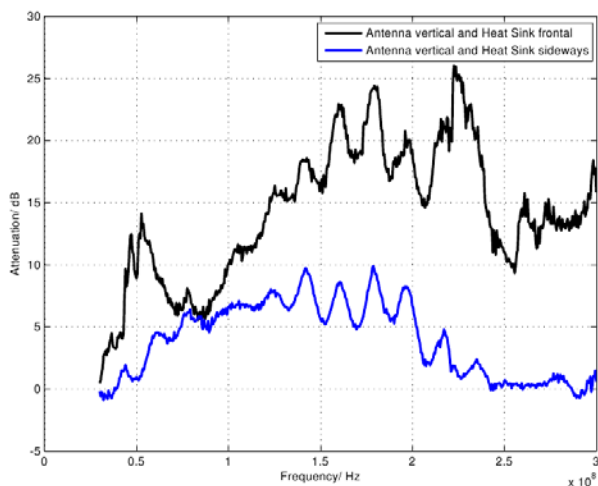


Figure 14 Attenuation of the heat sink ferrite model in the frequency range for frontal and lateral measurements [10]

The results of the radiation measurement show the attenuation of the heat sink ferrite model in the frequency range for frontal and lateral measurements of the heat sink in Fig. 14. The average attenuation value and the maximum attenuation value for the frontal are nearly 20 dB and 25 dB, respectively.

6. Conclusion

In this paper we discussed the influence of heat sink geometry on the input impedances of the heat sinks and their radiated emissions. Both values were measured for commercially available heat sinks and were used for reference purposes. Additionally, the alteration of a heat sink by placing a ferrite core between transistor and heat sink was investigated. This proved to be good method for the suppression of interfering currents in the heat sink due to a much larger input impedance. We found that in the relevant frequency range the input impedance is up to 45 dB above the impedance of unaltered heat sinks. This effect was explained using an equivalent circuit diagram. As a second effect, radiated emission from the heat sink is attenuated by the ferrite. Again, our proposals were validated by measuring the effect and comparing it with the emissions from an unaltered heat sink.

Acknowledgement

The authors would like to thank Dr. H. Fischer, Dr. J. Kolbe, Dr. L. Fichte, D. Peppel, T. Kut and B. Schetelig for the fruitful discussions during the research.

References

- [1] Damiano, A., Gatto, G., Marongiu, I., and Piroddi, A.: A heat sink model for EMI resonance frequency determination, Power Electronics Specialists Conference, vol. 1, pp. 273–277, 2004.
- [2] Dawson, J.F., Marvin, A.C., Porter, S.J., Nothofer, A., Will, J.E., Hopkins, S.: The effect of grounding on radiated emissions from heatsinks, IEEE International Symposium on Electromagnetic Compatibility, vol.2, pp. 1248-1252, 2001.

- [3] Li, R. and Zhang, L.-C.: Heatsink grounding effect on radiated emission of electronic device, 3rd International Symposium on Electromagnetic Compatibility, pp. 704–709, 2002.
- [4] Tihanyi, L.: Electromagnetic Compatibility in Power Electronics, J.K. Eckert & Company, Inc., Sarasota, Florida, 1995.
- [5] Felic, G. and Evans, R.: Study of heat sink EMI effects in SMPS circuits, IEEE International Symposium on Electromagnetic Compatibility, vol. 1, pp. 254–259, 2001.
- [6] Nagel, A.: Leitungsgebundene Störungen in der Leistungselektronik: Entstehung, Ausbreitung und Filterung [Dissertation], Wissenschaftsverlag, Mainz, 2001.
- [7] Samir, A. and Fujiwara, O.: Calculation of load effect produced by ferrite core attached to wire above a ground plane, Asia Pacific Microwave Conference, vol. 1, 1999.
- [8] Das, S. and Roy, T.: An investigation on radiated emissions from heatsinks, IEEE International Symposium on Electromagnetic Compatibility, vol. 2, pp. 784–789, 1998.
- [9] Diepenbrock, J., Archambeault, B., and Hobgood, L.: Improved grounding method for heat sinks of high speed processors, Electronic Components and Technology Conference, pp. 993–996, 2001.
- [10] J. Kulanayagam, J. H. Haggmann, Klaus F. Hoffmann, S. Dickmann.: Reduction of Heat Sink Common Mode Currents in SMPS Circuits, Advances in Radio Sciences, 2010.